BLIND IMAGE QUALITY EVALUATION USING PERCEPTION BASED FEATURES

Venkatanath N*, Praneeth D*, Maruthi Chandrasekhar Bh*, Sumohana S. Channappayya†, and Swarup S. Medasani*
*Image Understanding Group, Uurmi Systems Pvt. Ltd., Hyderabad
†Department of Electrical Engineering, Indian Institute of Technology Hyderabad

***Abstract*—This paper proposes a novel no-reference Perception-based Image QUality Evaluator (PIQUE) for real-world imagery. A majority of the existing methods for blind image quality assessment rely on opinion-based supervised learning for quality score prediction. Unlike these methods, we propose an opinion unaware methodology that attempts to quantify distortion without the need for any training data. Our method relies on extracting local features for predicting quality. Additionally, to mimic human behavior, we estimate quality only from perceptually significant spatial regions. Further, the choice of our features enables us to generate a fine-grained block level distortion map. Our algorithm is competitive with the state-of-the-art based on evaluation over several popular datasets including LIVE IQA, TID & CSIQ. Finally, our algorithm has low computational complexity despite working at the block-level.**

Keywords*—*No reference image quality assessment, spatial activity, Perceptual quality

I. INTRODUCTION

Increasing trends in multimedia content sharing over social networking sites and video streaming over the internet has precipitated the need to disseminate image content of high perceptual quality. Since in most such cases, there is no access to the original/uncompressed image data, one cannot estimate the quality of the received image relative to the reference or pristine image, thus rendering full reference methods to be of little use. Therefore, there is an acute need for an efficient Blind/No-Reference Image Quality Assessment (B/NR-IQA) algorithm for accurately estimating the perceptual quality of images. In this context, NR-IQA has been an important area of research in the recent past. The approaches to NR-IQA can be categorized based on the requirement of training data (Subjective or Objective quality scores) and apriori knowledge of distortion. In the following, we broadly show how the state-of-the-art methods fall into one of these categories.

The algorithms in [1], [2], [3], [4], [5] require prior information about the type of distortion (like JPEG, JPEG2000, Blur, ringing, etc.) for estimation of image quality. The algorithms in [6], [7], [8], [9], [10], [11], [12], [13], [14], [15] do not require such prior information about distortion types.

Some of these methods have trained their features using human subjective scores [6], [7], [8], [9], [13], [15], while others [10], [12], [14] have used objective scores derived from applying distortions to pristine images. There is also a class of methods that do not require either training data or distortion information as in [11]. These methods are truly blind in their approach to NR-IQA.

978-1-4799-6619-6/15/$31.00

In this paper, we propose an approach that does not involve any statistical learning (either from subjective or objective scores) for assessing image quality. Our goal is to estimate the amount of distortion present in a given test image, solely based on the local block/patch level characteristics of the test image. To address this challenging problem, we have taken cues from human perception of distortions. We attempt to classify a given block as a distorted block or not and assign a score accordingly. In addition to predicting quality, our method generates a fine-grained block-level spatial quality mask that is in turn useful for many other applications like feature point extraction, object detection, and compression.

The rest of the paper is organized as follows. Section II gives a brief background of the related work in this area. Section III provides details of the proposed approach for blind image quality assessment. In Section IV, the experimental framework and results of our method on different datasets are presented. A performance comparison with relevant state-of-the-art methods is also reported. Section V provides the conclusions and direction for future work.

II. BACKGROUND

In this section, we present a brief review of the state-of-the-art NR-IQA methods. In [6], Moorthy et al. proposed the Blind Image Quality Index (BIQI) algorithm, that uses statistical features computed from the wavelet coefficients of input images. As an enhancement to this work, Moorthy et al. in [7] proposed the Distortion Identification-Based Image Verity and Integrity Evaluation (DIIVINE) algorithm that uses 88 features and a two-stage classification framework for quality estimation. However, due to its computational complexity, real-time implementation is not possible. Saad et al. in [8] presented the Blind Image Integrity Notator Using DCT Statistics-II (BLIINDS-II) algorithm that uses generalized statistical model parameters derived from local DCT coefficients to estimate the quality of an image. In [9], Mittal et al. presented Blind/Referenceless Image Spatial Quality Evaluator (BRISQUE), a fast algorithm that uses 36 statistical features based on Natural Scene Statistics (NSS)-based model in spatial domain to perform quality estimation and distortion identification. It out performs DIIVINE and BLIINDS-II in both performance and computation time. In [10], Mittal et al. proposed an algorithm that conducts Probabilistic latent semantic analysis (pLSA) on the statistical features of a large collection of pristine and

distorted image patches. This technique does not use human subjective scores for training but relies on the learned features extracted from pristine and distorted patches to estimate quality score. Mittal et al. in [11] proposed the Naturalness Image Quality Evaluator (NIQE) algorithm that uses quality aware NSS features extracted only from a collection of pristine image patches to estimate quality. Xue et al. in [12] proposed a Quality-Aware Clustering (QAC) algorithm that learns a set of quality-aware centroids from pristine and distorted imagery and uses them as codebooks to infer the quality of a test image. Le, et al. in [13] proposed a Convolutional Neural Networks for No-Reference Image Quality Assessment (CNN-NRIQA) that works in spatial domain wihtout using handcrafted features for predicting image quality. Peng et al. in [14] proposed a Blind Learning of Image Quality using Synthetic Scores (BLISS) algorithm that trained a model using synthetic scores instead of using human opinion scores. Huixuan et al. in [15] proposed Blind Image Quality Assessment using semi-supervised rectifier networks algorithm that generalizes across a large set of images and distortion types without the need for a large amount of labeled data. Except QAC [12] and CNN-NRIQA [13], none of the other NR-IQA methods provide a spatial quality map of the input image. In this paper, we present a perception-based, block-level, blind approach in the spatial domain to estimate quality.

III. PROPOSED APPROACH

Our method is inspired from the following two principles about how humans perceive image quality. Firstly, humans visual attention is highly directed towards salient points in an image or spatially active regions. Secondly, local quality at block/patch level adds up to the overall quality of an image as perceived by humans. In our approach, the first principle is addressed by estimating distortion only on regions of spatial prominence and the second, by computing distortion levels at the local block level of size $n \times n$, where $n = 16$. Working at the block level would enable us to exploit the local characteristics that account for overall perceptual quality of an image.

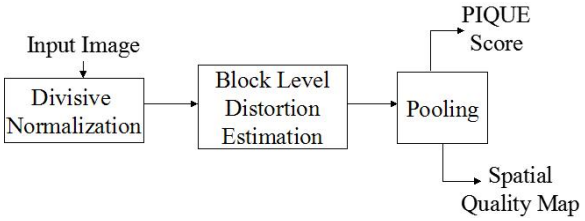

Fig. 1. Block Diagram of the proposed approach

Fig. 1 shows the block diagram of the proposed approach. The input image is subjected to a preprocessing step. Block level analysis is then performed for distortion identification. Each distorted block is assigned a score, based on the type of distortion. The block level scores are then pooled to determine the overall image quality. In addition to the quality score, a spatial quality map is also generated that can be used effectively by other applications. We describe each of these stages in the following sub-sections.

A. Divisive Normalization

The first pre-processing step that is performed on the input test image is local mean removal and divisive normalization. This step extracts Natural Scene Statistics (NSS) features from the grayscale image as explained in [16]. Such an operation is applied to luminance image $I(i,j)$ to produce:

$$\hat{I}(i,j) = \frac{I(i,j) - \mu(i,j)}{\sigma(i,j) + C}, \tag{1}$$

where $i \in 1, 2.....M$, $j \in 1, 2.....N$ are spatial indices, M, N are the image height and width respectively, C is constant, that is set to 1 to prevent instability and where

$$\mu(i,j) = \sum_{k=-K}^{K} \sum_{l=-L}^{L} w_{k,l} I_{k,l}(i,j) \tag{2}$$

$$\sigma(i,j) = \sqrt{\sum_{k=-K}^{K} \sum_{l=-L}^{L} w_{k,l} (I_{k,l}(i,j) - \mu(i,j))^2}, \tag{3}$$

In (2) and (3) $w = \{w_{k,l} | k = -K, \ldots, K, l = -L, \ldots, L\}$ is a 2D circularly symmetric Gaussian weighting function sampled out to 3 standard deviations (K = L = 3) and rescaled to unit volume. The transformed luminance values of (1) are called Mean Subtracted Contrast Normalized (MSCN) coefficients. We refer the reader to BRISQUE IQE model [9] for a detailed exposition on this process.

The input image is segmented into non-overlapping blocks, Bk of size, $n \times n$ leaving out those at the image boundaries on all four sides. The MSCN coefficients are utilized to label a given block either as a uniform (U) block or as a non-uniform/spatially active (SA) blocks. The criterion to label a block is given below.

$$B_k = \begin{cases} U & \nu_k < T_U \\ SA & \nu_k \geq T_U. \end{cases} \tag{4}$$

where ν_k is the variance of the MSCN coefficients, $\hat{I}(i,j)$ in a given block, B_k, $k \in 1, 2, \ldots, N_B$. N_B is the total number of blocks of size $n \times n$ with n=16 in our case. Through empirical observations, we set threshold T_U as equal to 10%. Since, we are computing the variance of normalized coefficients that varies from 0 to 1, it is treated as a percentage. The empirical observations correlate well perceptually also, where-in one would expect the variance of MSCN coefficients to be low for blocks with low spatial activity. Blocks with considerable or high spatial activity would have variance greater than 0.1 (which effectively means 10%).

B. Block Level Distortion Estimation

The most common distortions affecting images are due to compression and transmission. The perceivable artifacts due to these distortions can broadly be classified into blockiness, blur and noise. In Fig. 2, we show the methodology for block level distortion classification and quantification for estimating a block score.

In our method, spatially active blocks, B_k are analysed for two types of distortion criteria, namely, noticeable distortion criterion and additive white noise criterion. A distorted block is

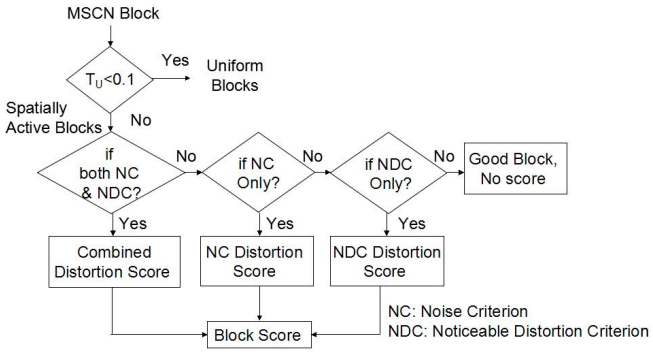

Fig. 2. Block level Distortion Classification and Quantification

then assigned a distortion score based on the type of distortion. In the following, we define the criteria to estimate whether a spatially active block is affected by distortions or not.

1) Noticeable Distortion Criterion: A block level distortion is noticeable if at least one of its edge segments (segment is defined as a collection of 6 contiguous pixels in a block edge) exhibits low spatial activity [17]. For a spatially active block, B_k derived from $\hat{I}(i,j)$ of size $n \times n$ with $n = 16$, each edge, L_p is divided into eleven segments as under:

$$a_{pq} = L_p(x) : x = q, q+1, \ldots, q+5, \tag{5}$$

where a_{pq} is the structuring element, p ϵ 1,2,3,4 denotes edge index, and q ϵ 1,2,3,...,11 denotes the segment index. The block and its edge segments are shown in Fig. 3. A segment exhibits low spatial activity if the standard deviation of the segment, a_{pq} is less than threshold T_{STD}.

$$\sigma_{pq} < T_{STD} \tag{6}$$

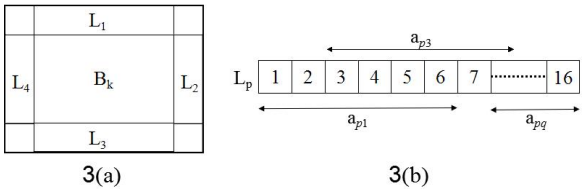

Fig. 3. (a). Block B_k, and its edges (b). Eleven segments of the edge, L_p.

In [17], the analysis is done on the luminance image, and for 8×8 block size. However, threshold determination becomes a difficult task when working with luminance images. To mitigate this issue, we work with MSCN coefficients that help in significantly reducing threshold variability. After performing experiments, we could arrive at empirical threshold for T_{STD} = 10%. A block is considered as distorted if at least one of its segments satisfies (6). The following sub-section explains the criterion used to classify and estimate noise in a given block.

2) Noise Criterion: Additional perception based center-surround criterion is considered here to model noise distortion using block level MSCN features. This criterion is inspired by the Human Visual System's (HVS) sensitivity to center-surround variations. We divide the block into two segments as shown in Fig. 4. One is the central segment that contains the center two columns, S_{cen}. The other segment, S_{sur} consists of the remaining columns.

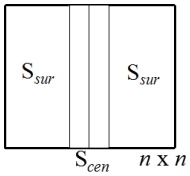

Fig. 4. Choice of center and surround regions in a block

On analysis, we found that there is a definitive relation between the center-surround deviation ratio and the block standard deviation of that MSCN block. We empirically modeled a parameter, β to quantify this relation:

$$\beta = \frac{|(\frac{\sigma_{cen}}{\sigma_{sur}}) - \sigma_{blk}|}{\max((\frac{\sigma_{cen}}{\sigma_{sur}}), \sigma_{blk})}, \tag{7}$$

where σ_{cen} is the standard deviation of segment, S_{cen}, σ_{sur} is the standard deviation of segment, S_{sur}, σ_{blk} is the standard deviation of spatially active block, B_k derived from $\hat{I}(i,j)$. Through Fig. 5, we try to explain the variation of β for varying noisy conditions. Fig. 5(a), Fig. 5(c) & Fig. 5(e) show the low, medium and high noisy images from LIVE Database. Fig. 5(b), Fig. 5(d) & Fig. 5(f) shows the distribution of β and σ_{blk} across blocks for the corresponding images in Fig. 5(a), Fig. 5(c) & Fig. 5(e) respectively. It can be observed from Fig. 5(b), Fig. 5(d) & Fig. 5(f) that as noise increases (low SNR conditions), β decreases and becomes almost zero for high noise cases. In high SNR conditions, β is almost equal to the block standard deviation, σ_{blk}. Thus, a given block, B_k can be categorized as affected with noise if it satisfies the below condition:

$$\sigma_{blk} > 2 * \beta. \tag{8}$$

3) Quantifying Distortion using Block Variance Parameter: Once we identify that a given block is distorted, the next step would be to quantify the amount of distortion contributed by that block to the overall score. Through our experiments, we could observe that the variance of the MSCN coefficients of a given block, ν_{blk} shows significant signature of the amount of distortion present in that block. This is illustrated in Fig. 6. Fig. 6(a) shows the high spatial activity image and Fig. 6(b), Fig. 6(c) & Fig. 6(d) show the variation of block variance of the MSCN coefficients of a JPEG compressed, blurred and AWGN images respectively. These images are taken from LIVE database. In Fig. 6(b) and Fig. 6(c) block variance is very low for highly distorted images as compared with medium and pristine images, indicating that variance is inversely proportional to the amount of distortion. However, this is not the case with noise distortion. Due to the additive nature of Gaussian noise, blocks affected by such a distortion cannot have low variance. Instead, the variance of such blocks is expected to increase with increasing noise. This was observed experimentally as well, as shown in the plot of Fig. 6(d). So, while quantifying noise using the same parameter variance, we need to understand that it is directly proportional to the amount of distortion.

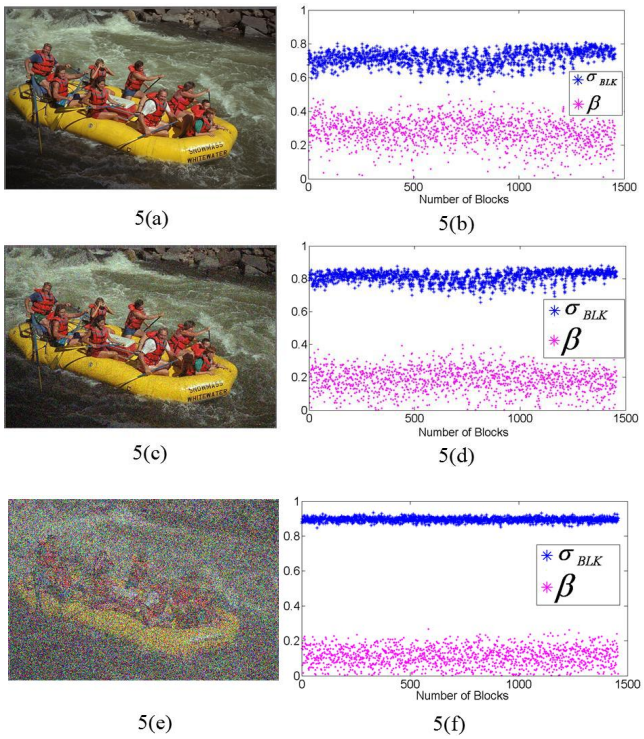

Fig. 5. (a). Low noise image (c). Medium noise image (e). High noise image (b), (d), (f): Corresponding σ_{blk} vs β plots.

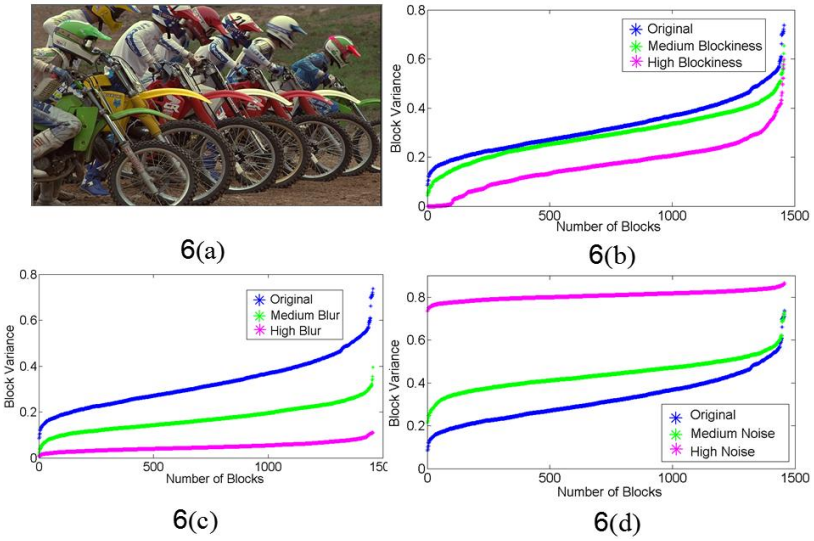

Fig. 6. (a). Bikes Reference Image from LIVE. (b). Variance plot for original and JPEG distortions. (c). Variance plot for original and Blur distortions. (d). Variance plot for original and AWGN distortions.

4) Pooling: We use variance feature, ν_{blk}, to assign the amount of distortion for a distorted block. The following is the distortion assigment procedure for a given block, B_k.

$$D_{sk} = \begin{cases} 1 & if \quad (6)\,\&\,(8) \\ \nu_{blk} & if \quad (8) \\ (1-\nu_{blk}) & if \quad (6). \end{cases} \tag{9}$$

Perception based Image Quality Evaluator, PIQUE is then given by:

$$PIQUE = \frac{\left(\sum_{k=1}^{N_{SA}} D_{sk}\right) + C_1}{(N_{SA} + C_1)}, \tag{10}$$

where N_{SA}, is the number of Spatially Active blocks in a given image, and where C_1 is a positive constant ($C_1 = 1$ in our case) that is included to prevent numerical instability when the denominator of (10) goes to 0. This is possible in cases of

high blur, where images get over smoothened resulting in no spatial activity. It can also be noted that the value of D_{sk} in any of the above cases, does not exceed the value of 1. As a result, the PIQUE score also lies in the range of 0 to 1, as per (10). If the PIQUE score is near to zero (0 to 0.3), it represents a good quality image. If it is near to 1, it refers to a poor quality image (0.5 to 1.0). If the PIQUE score lies in between 0.3 to 0.5 it can be treated as an average quality image. In the whole process of PIQUE index calculation, only one threshold has been used at two places (4) & (6). This variance threshold (T_U or T_{STD}) is used essentially to determine whether a given block or a block-edge-segment exhibits low spatial activity. However, the distortion analysis at these two places is handled differently as explained in the algorithm.

IV. EXPERIMENTS AND RESULTS

In this section, we report the performance of our algorithm on most of the publicly available benchmark databases. Also, the effect of changing thresholds on the performance of the method is reported.

A. Experimental Framework and Results

The performance of PIQUE is evaluated on three of the largest publicly available databases that have human subjective scores, LIVE [18], CSIQ [19] and TID2008 [20]. Tables I, II, III report the correlation scores (SROCC [21] & PCC [21]) of PIQUE, QAC [12] and NIQE [11] on three databases, LIVE, CSIQ and TID respectively. Table I shows that the proposed metric, PIQUE performed well over QAC and NIQE both in terms of SROCC and PCC on LIVE IQA database. Even on CSIQ and TID databases, PIQUE is very competitive to QAC and NIQE and performed consistently better for White Noise in terms of both SROCC and PCC. Fast Fading (FF) was not considered in the above reports for consistency and comparison with QAC & NIQE.

In addition to a distortion score to the image, our algorithm also generates a spatial quality mask. The mask generated by our method is more fine-graded (Block size=16×16) than that reported in QAC [12]. Additionally, PIQUE mask also identifies the type of dominant distortion that is available at the block level as shown in Fig. 7. To demonstrate this block level distortion analysis capability of PIQUE, a JP2K distorted image from LIVE database is taken and AWGN noise is added to the cloudy patches. This distorted image along with its corresponding spatial quality mask as generated by PIQUE are shown in Fig. 7. Green fill indicates uniform-block that is not considered for analysis. Red and Yellow fills indicate blocks that satisfy (6) & (8) respectively. Spatially active blocks that are not affected by any distortion are not filled with any color. This can also be perceptually corroborated.

1) Effect of T_U and choice of block size: In this sub-section, we discuss the effect of varying T_U and choice of block size on the performance of the metric. Table IV shows the SROCC scores for LIVE database with varying T_U (Spatial activity threshold) in steps of 5 from 5% to 30%. It can be observed that, significant performance variations are not seen in the range from 5% to 20%. Table V shows the SROCC scores for LIVE database with varying block sizes from 16×16 to 96×96 with step size of 16. It can be noted that for block sizes greater than 32×32, there is a drop in the performance of the algorithm. This indicates that the selected criteria capture distortions only at smaller block sizes. It can thus be noted from these results that local characteristics at the block level play a prominent role in quality prediction.

B. Computational Time

Though we are analyzing local characteristics at block level, in most of the cases, we are using only standard deviation & variance as the parameters for distortion identification and evaluation. Also, since our metric is content dependent, the timing varies from image to image. We report here in Table VI, the average execution time (in MATLAB) of our metric per image when tested on the complete LIVE Database (808 images). We used a PC with Intel Core-i3-2100 CPU and 2 GB RAM. Our metric can be used in real-time applications with optimized C implementation for SVGA resolution images at 33 FPS. Table VI also shows execution time comparison with other IQA techniques.

V. CONCLUSIONS AND FUTURE WORK

In this paper, we presented a completely blind NR-Quality Evaluation Metric that uses cues from human visual system to address the problem of blind image quality assessment. PIQUE scores correlate well with human subjective scores of three different databases. The algorithm is moderately fast and can be used in real-time applications. Additionally, the block-level analysis presented here helps in the generation of a distortion identifying spatial quality mask that is useful in many other applications.

We are currently working towards addressing the scenario where a given block is affected by more than one distortion using a weighted combination of scores for each of the component distortions. We believe that such an approach would be more effective in handling realistic distortion scenarios. Further, we are working on demonstrating the utility of the distortion mask in various task dependent quality assessment applications.

SROCC					
Algorithm	JP2K	JPEG	WN	Blur	All
QAC	0.85	0.94	0.96	0.91	0.89
NIQE	0.91	0.85	0.97	0.94	0.88
PIQUE	*0.93*	*0.89*	*0.96*	*0.92*	*0.91*
Pearson CC					
QAC	0.85	0.94	0.96	0.91	0.89
NIQE	0.91	0.85	0.97	0.94	0.88
PIQUE	*0.93*	*0.90*	*0.94*	*0.90*	*0.90*

TABLE I. LIVE DATABASE

SROCC					
Algorithm	JP2K	JPEG	WN	Blur	All
QAC	0.87	0.91	0.86	0.85	0.86
NIQE	0.89	0.86	0.81	0.87	0.86
PIQUE	*0.87*	*0.86*	*0.91*	*0.86*	*0.84*
Pearson CC					
QAC	0.90	0.94	0.87	0.84	0.88
NIQE	0.90	0.91	0.81	0.89	0.86
PIQUE	*0.90*	*0.88*	*0.93*	*0.88*	*0.87*

TABLE II. CSIQ DATABASE

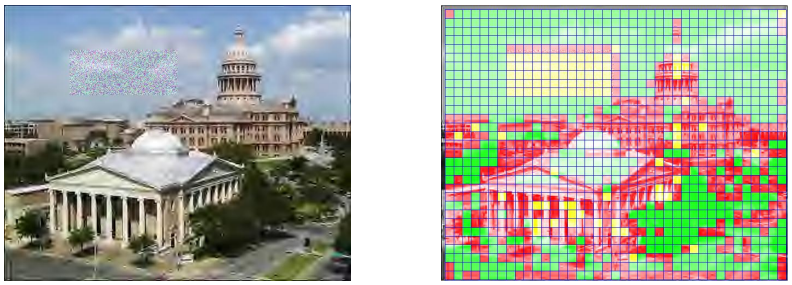

Fig. 7. JP2K Distorted Image from LIVE Database with added AWGN noise patch & its PIQUE Spatial Quality Mask. Where Red, Yellow and Green fill indicates blocks that satisfy NDC, NC and uniform criterions.

SROCC					
Algorithm	JP2K	JPEG	WN	Blur	All
QAC	0.89	0.90	0.71	0.85	0.87
NIQE	0.89	0.88	0.78	0.82	0.80
PIQUE	*0.93*	*0.83*	*0.78*	*0.85*	*0.85*
Pearson CC					
QAC	0.88	0.92	0.72	0.85	0.84
NIQE	0.90	0.92	0.77	0.84	0.80
PIQUE	*0.93*	*0.87*	*0.78*	*0.84*	*0.86*

TABLE III. TID DATABASE

SROCC					
Distortion/T_U	JP2K	JPEG	WN	Blur	All
0.05	0.92	0.88	0.96	0.92	0.90
0.1	0.93	0.89	0.96	0.92	0.91
0.15	0.92	0.89	0.96	0.91	0.91
0.2	0.89	0.88	0.96	0.86	0.88
0.25	0.84	0.86	0.96	0.82	0.84
0.3	0.76	0.83	0.96	0.81	0.79

TABLE IV. SROCC SCORES FOR LIVE DATABASE WITH VARYING T_U

SROCC					
Block Size	JP2K	JPEG	WN	Blur	All
16×16	0.93	0.89	0.96	0.92	0.91
32×32	0.92	0.89	0.94	0.93	0.88
48×48	0.90	0.87	0.93	0.93	0.83
64×64	0.89	0.85	0.90	0.93	0.81
80×80	0.87	0.81	0.88	0.92	0.78
96×96	0.88	0.81	0.84	0.91	0.76

TABLE V. SROCC SCORES FOR LIVE DATABASE WITH VARYING BLOCK SIZE

Method	QAC	NIQE	PIQUE	DIIVINE	BLIINDS-II
Time (sec)	0.2	0.8	0.9	60	140

TABLE VI. MATLAB EXECUTION TIME

REFERENCES

[1] H. Sheikh, A. Bovik, and L. Cormack, "No-reference quality assessment using natural scene statistics: Jpeg2000," *Image Processing, IEEE Transactions on*, vol. 14, no. 11, pp. 1918 –1927, nov. 2005.

[2] P. Marziliano, F. Dufaux, S. Winkler, and T. Ebrahimi, "Perceptual blur and ringing metrics: application to jpeg2000," *Signal Processing: Image Communication*, vol. 19, no. 2, pp. 163–172, 2004.

[3] Z. Wang, H. Sheikh, and A. Bovik, "No-reference perceptual quality assessment of jpeg compressed images," in *Image Processing. 2002. Proceedings. 2002 International Conference on*, vol. 1, 2002, pp. I–477 – I–480 vol.1.

[4] T. Vlachos, "Detection of blocking artifacts in compressed video," *Electronics Letters*, vol. 36, no. 13, pp. 1106–1108, 2000.

[5] Z. Wang, A. C. Bovik, and B. Evan, "Blind measurement of blocking artifacts in images," in *Image Processing, 2000. Proceedings. 2000 International Conference on*, vol. 3. Ieee, 2000, pp. 981–984.

[6] A. K. Moorthy and A. C. Bovik, "A two-step framework for constructing blind image quality indices," *Signal Processing Letters, IEEE*, vol. 17, no. 5, pp. 513–516, 2010.

[7] A. Moorthy and A. Bovik, "Blind image quality assessment: From natural scene statistics to perceptual quality," *Image Processing, IEEE Transactions on*, vol. 20, no. 12, pp. 3350 –3364, dec. 2011.

[8] M. A. Saad, A. C. Bovik, and C. Charrier, "Blind image quality assessment: A natural scene statistics approach in the dct domain," *Image Processing, IEEE Transactions on*, vol. 21, no. 8, pp. 3339–3352, 2012.

[9] A. Mittal, A. Moorthy, and A. Bovik, "No-reference image quality assessment in the spatial domain," *Transactions on Image Processing, IEEE*, vol. 21, no. 12, pp. 4695 – 4708, Dec. 2012.

[10] A. Mittal, G. S. Muralidhar, J. Ghosh, and A. C. Bovik, "Blind image quality assessment without human training using latent quality factors," *Signal Processing Letters, IEEE*, vol. 19, no. 2, pp. 75–78, 2012.

[11] A. Mittal, R. Soundararajan, and A. Bovik, "Making a completely blind image quality analyzer," *Signal Processing Letters, IEEE*, vol. 20, no. 3, pp. 209 – 212, Mar. 2013.

[12] W. Xue, L. Zhang, and X. Mou, "Learning without human scores for blind image quality assessment," in *Computer Vision and Pattern Recognition (CVPR), 2013. IEEE Conference on*. IEEE, 2013, pp. 995–1002.

[13] P. Y. Y. L. Kang, Le and D. Doermann, "Convolutional neural networks for no-reference image quality assessment," in *Computer Vision and Pattern Recognition (CVPR)*, 2014.

[14] J. K. Ye, Peng and D. Doermann, "Beyond human opinion scores: Blind image quality assessment based on synthetic scores," in *Computer Vision and Pattern Recognition (CVPR)*, 2014.

[15] N. J. Tang, Huixuan and A. Kapoor, "Blind image quality assessment using semi-supervised rectifier networks," in *Computer Vision and Pattern Recognition (CVPR)*, 2014.

[16] D. L. Ruderman, "The statistics of natural images," *Network: computation in neural systems*, vol. 5, no. 4, pp. 517–548, 1994.

[17] R. V. Babu, A. S. Bopardikar, A. Perkis, and O. I. Hillestad, "No-reference metrics for video streaming applications," in *International Workshop on Packet Video*, 2004.

[18] H. Sheikh, Z. Wang, L. R. Cormack, and A. C. Bovik, "Live image quality assessment database release 2."

[19] E. C. Larson and D. M. Chandler, "Most apparent distortion: full-reference image quality assessment and the role of strategy," *Journal of Electronic Imaging*, vol. 19, no. 1, pp. 011 006–011 006, 2010.

[20] N. Ponomarenko, V. Lukin, A. Zelensky, K. Egiazarian, M. Carli, and F. Battisti, "Tid2008-a database for evaluation of full-reference visual quality assessment metrics," *Advances of Modern Radioelectronics*, vol. 10, no. 4, pp. 30–45, 2009.

[21] V. Q. E. Group *et al.*, "Final report from the video quality experts group on the validation of objective models of video quality assessment," *VQEG, Mar*, 2000.